ISAS - INTERNATIONAL SCHOOL
FOR ADVANCED STUDIES

T E S I

DIPLOMA DI PERFEZIONAMENTO

"MAGISTER PHILOSOPHIAE"

THEORY OF SPIN-POLARIZED SECONDARY ELECTRON EMISSION

CANDIDATO:
J. Glazer

Relatore:
Prof. E. Tosatti

Anno Accademico 1982/1983

TRIESTE

SISSA - SCUOLA
INTERNAZIONALE
SUPERIORE
STUDI AVANZATI
TRIESTE
Strada Costiera 11

SCUOLA INTERNAZIONALE SUPERIORE DI STUDI AVANZATI

TRIESTE

Tesi di Master

THEORY OF SPIN-POLARIZED SECONDARY ELECTRON EMISSION

Settore: Stati Condensati della Materia

Supervisore: Prof. Erio Tosatti

Candidato: Jerzy Glazer

Anno Accademico: 1982-1983

Abstract

A simple spin-polarized parabolic band model of a metal is used as the basis for a computer simulation of the cascade leading to secondary electrons' emission.For a paramagnetic metal,spin-flip processes are found to give rise to a slight negative polarisation of secondaries for a totally polarized primary beam.In a ferromagnetic metal repeated inelastic scattering leads to spin polarization parallel to the internal moment.The role of two mechanisms: a) difference between mean-free-paths of spin-up and spin-down electrons and b) spin-flip due to exchange scattering is clarified.

1. Introduction

When an energetic primary electron is injected into a metal will lose its energy via electron-hole (e-h) pair creation. The electrons excited above the Fermi level in this process travel through the metal being scattered both elastically (e.g., Bragg-diffracted by the lattice) and inelastically, by giving rise to further e-h pairs. Some of these electrons can eventually leave the metal, by crossing its surface. Those electrons which leave after so many inelastic scatterings events that their energy is reduced to only a few eV are the secondaries.

The theory of secondaries was first tackled some 30 years ago [1]. So far, however, the spin properties of secondaries have not been given any theoretical discussion. On the other hand spin-resolved experiments on secondaries have appeared quite recently [2-5].

There are three basic steps involved in a spin-polarized calculation of secondaries.

The first is the determination of cross-section for a single scattering event. For a given initial energy E and energy loss ω ($<E$), there are two such cross-sections in a paramagnetic metal: non-flip, and spin-flip, and corresponding four of them in a ferromagnetic metal. The calculation of these scattering rates is presented in section II, (following the work of Yin and Tosatti [6] and Yin, Tosatti and Glazer [7]) based on the simple parabolic band model.

The second step is to generate the cascade of inelastic scattering events. A quantum-mechanical treatment of a large number of scattering events including overall phase coherence is in practice out of the question. It is clear, however, that to some extent such a level of complication is excessive. For increasing electron energies, for example, quantum-mechanical interference between products of different scattering events should rapidly become negligible - we shall assume that they can in fact be neglected throughout, thereby going from scattering amplitudes to probabilities.

With this crucial approximation, the cascade formation can be simulated on the computer: the electrons are treated as classical objects, that follow a trajectory determined in each case by a series of single scattering events, whose individual probabilities are the (quantum--mechanical!) cross-sections determined above. This computer simulation is described in section III.

The third, and last step in the generation of actual secondaries is escape through the surface.

In the optical approximation [8] the potential felt by an electron in the solid is constant and has a real and an imaginary part corresponding to refraction and energy loss respectively. Escape through the surface in our model is described accurately by refraction alone. An electron escaping to the vacuum diminishes its energy by decreasing the momentum component perpendicular to the surface. When this component is too small the electron turns back being elastically scattered (total reflection). When the normal moment component is larger than the threshold value $\sqrt{2m(\phi+E_F)/h^2}$ escape becomes possible.

2. Theory of spin scattering inelastic rates

We use a model of paramagnetic or ferromagnetic metal consisting of a single parabolic band for each spin filled up to the common Fermi level E_F (Fig.1).

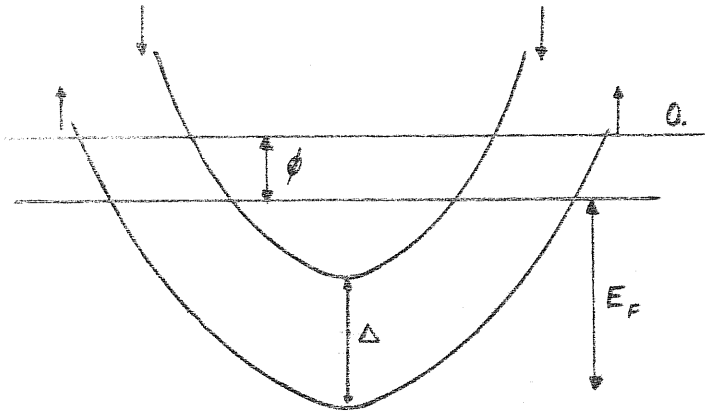

Fig.1: A simple model of ferromagnetic iron with majority of spin-up electrons. Here the energy zero is that of vacuum, ϕ is the work function, E_F is the Fermi energy and Δ is the exchange splitting (Δ=0 for a paramagnet).

The model is described by three parameters: the Fermi energy, the exchange splitting between spin-up and spin-down (for a paramagnet Δ=0), and the work function ϕ, the minimal energy required to excite electron from the Fermi level to the vacuum (see Fig.1). The values of E_F and Δ are determined by conduction electron density n and bulk polarization P_B. Calling $n^{\uparrow(\downarrow)}$ the density of spin-up(down) electrons, we have (we use for convenience $\hbar$=1.):

$$\frac{n^{\uparrow} - n^{\downarrow}}{n} = P_B \qquad (1)$$

$$n^{\uparrow} = (2mE_F)^{3/2}/6\pi^2 \qquad (2)$$

$$n^{\downarrow} = (2m(E_F-\Delta))^{3/2}/6\pi^2 \qquad (3)$$

where m is the electron mass. Adding the obvious condition:

$$n^{\uparrow} + n^{\downarrow} = n \qquad (4)$$

we end up with a complete set of equations which give for fixed n and P_B the values of E_F and Δ. The work function ϕ is given the fixed value 4.3eV, to simulate Al (paramagnetic) or Fe (ferromagnetic).

We shall denote by $R_f^{\uparrow}(E,\omega)$ the probability per unit time that the incoming spin-up electron, with energy E, will, by a simple scattering event, lose energy ω and flip to spin-down, and by $R_{nf}^{\downarrow}(E,\omega)$ the similar process without spin-flip. $R_f^{\downarrow}(E,\omega)$, $R_{nf}^{\downarrow}(E,\omega)$ are the same quantities for incoming spin-down electron. Obviously, for $\Delta=0$ $R_f^{\uparrow}=R_f^{\downarrow}$, $R_{nf}^{\uparrow}=R_{nf}^{\downarrow}$. The energy E is conventionally measured with respect to the Fermi level. All those quantities have been calculated in Ref. [6] and [7]. We briefly recall here the general scheme.

The scattering rate of the electron from the state $\underline{p}^{\uparrow}$,E(p) ($\underline{p}^{\uparrow}$-momentum of spin-up electron) to the final state $(\underline{p}-\underline{q})^{\downarrow}$,E(p)-$\omega$ with the momentum transfer $\underline{q}$ and energy transfer ω between antiparallel spin electrons is proportional in lowest order perturbation theory to the imaginary part of the forward scattering amplitude, that is according to Fig.(2) [9]:

$$R_f^{\uparrow}(\omega) = \frac{1}{2\pi^3}\left(\frac{e^2 p_F^{\uparrow}}{2E_F}\right)^2 \int d^3q \int d^3k \cdot \frac{\Theta(|\underline{k}+\underline{q}|-1)}{\left((\underline{p}-\underline{q}-\underline{k})^2 + q_{FT}^2\right)^2} \times$$

$$\times\, \Theta((1-2\Delta)^{1/2}-k).\, \delta(\underline{p}.\underline{q} - q^2/2 - \Delta - \omega).\, \delta(\underline{q}.\underline{k} + q^2/2 - \Delta - \omega) \qquad (5)$$

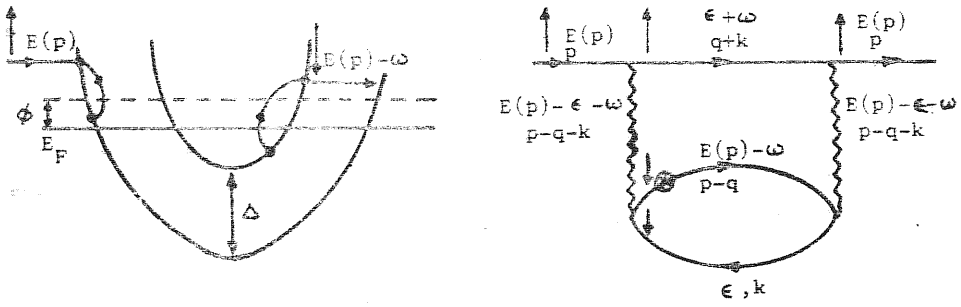

Fig.2. (a)&(b):spin-flip process for an incoming electron with spin parallel to the majority spin electrons.Left panel: band picture. Right panel: Feynman diagram.

All the momenta and energies are expressed in the terms of $p_F^{\uparrow}$ and $2E_F$ respectively, where $p_F^{\uparrow}=\sqrt{2mE_F}$.

As an interaction between electrons we adopt a statically screened coulomb interaction:

$$V(q) = \frac{4\pi e^2}{q^2 + q_{FT}^2} \qquad (6)$$

where q_{FT} is the Thomas-Fermi static screening length given by $q_{FT}=(6\pi n e^2/E_F)^{1/2}$ and e is the electron charge.

The rational for this choice is discussed in [6] & [7] and is roughly as follows. True lowest order perturbation theory would imply a bare coulomb interaction $V(q)=4\pi e^2/q^2$. Full summation of the RPA bubble series would instead yield, $V_{RPA}(q,\omega)=4\pi e^2/q^2\sqrt{\epsilon_{RPA}(q,\omega)}$. This expression is more accurate - in particular, it does take into account excitation of plasmons - but has disadvantages for a practical calculation, in that it depends simultaneously and not too simply upon both q and ω.

A statically screened form like (6) is less accurate but not too unrealistic, except for ω close to plasmon frequencies. The plasmon oscilator strength is shifted, with this replacemant, for $\omega\sim\omega_p$, to $\omega\sim E_F$; i.e. to electron-hole pairs. For our purpose, this is good enough on two accounts:(i) spin-polarization from plasmon scattering is known to be insignificant [10], (ii) for densities such as those of Al or Fe, ω_p and E_F are numerically not very different.

The probability $R_f^{\uparrow}(E,\omega)$ is obtained, as shown in equation (5), by summing over all possible momenta $\underline{q}$ transferred to excited electron and all possible momenta $\underline{k}$ of the hole left below the Fermi level. In the same way the non-flip rate $R_{nf}^{\uparrow}$ can be calculated, but in this case more diagrams have to be considered:

$$R_{nf}^{\uparrow}(E,\omega)=R_{nf1}^{\uparrow}(E,\omega)+R_{nf2}^{\uparrow}(E,\omega)+R_{nf3}^{\uparrow}(E,\omega)+2R_{nf4}^{\uparrow}(E,\omega) \qquad (7)$$

where:

$$R_{nf1}^{\uparrow}(\omega) = \frac{1}{2\pi^3}\left(\frac{e^2 p_F^{\uparrow}}{2E_F}\right)^2 \int d^3q \int d^3k \; \frac{\Theta\left((1-2\Delta)^{1/2}-k\right)}{\left(q^2+q_{FT}^2\right)^2} \times \qquad (8)$$

$$\times\, \Theta(|q+k|-(1-2\Delta)^{1/2}).\,\delta(\underline{p}.\underline{q}-q^2/2-\omega).\,\delta(\underline{q}.\underline{k}+q^2/2-\omega)$$

$$R_{nf2}^{\uparrow}(\omega) = \frac{1}{2\pi^3}\left(\frac{e^2 p_F^{\uparrow}}{2E_F}\right)^2 \int d^3q \int d^3k \; \frac{\Theta(|\underline{q}+\underline{k}|-1)}{\left(q^2+q_{FT}^2\right)^2} \times \qquad (9)$$

$$\times\, \Theta(1-k).\,\delta(\underline{p}.\underline{q}-q^2/2-\omega).\,\delta(\underline{q}.\underline{k}+q^2/2-\omega)$$

$$R^{\uparrow}_{nf3}(\omega) = \frac{1}{2\pi^3}\left(\frac{e^2 p_F^{\uparrow}}{2E_F}\right)^2 \int d^3q \int d^3k \, \frac{\Theta(|\underline{q}+\underline{k}|-1)}{\left((\underline{p}-\underline{q}-\underline{k})^2 + q_{FT}^2\right)^2} \times \tag{10}$$

$$\times\, \theta(1-k).\, \delta(\underline{p}.\underline{q} - q^2/2 - \omega).\, \delta(\underline{q}.\underline{k} + q^2/2 - \omega)$$

$$R^{\uparrow}_{nf4}(\omega) = \frac{-1}{2\pi^3}\left(\frac{e^2 p_F^{\uparrow}}{2E_F}\right)^2 \int d^3q \int d^3k \, \frac{\Theta(|\underline{q}+\underline{k}|-1)}{(q^2 + q_{FT}^2).\left((\underline{p}-\underline{q}-\underline{k})^2 + q_{FT}^2\right)} \times \tag{11}$$

$$\times\, \theta(1+k).\, \delta(\underline{p}.\underline{q} - q^2/2 - \omega).\, \delta(\underline{q}.\underline{k} + q^2/2 - \omega)$$

The negative $R^{\uparrow}_{nf4}$ term represents the exchange process present only in a non-flip rate. As an example we display on Fig.3 diagrams associated with $R^{\uparrow}_{nf1}$ and $R^{\uparrow}_{nf2}$ terms.

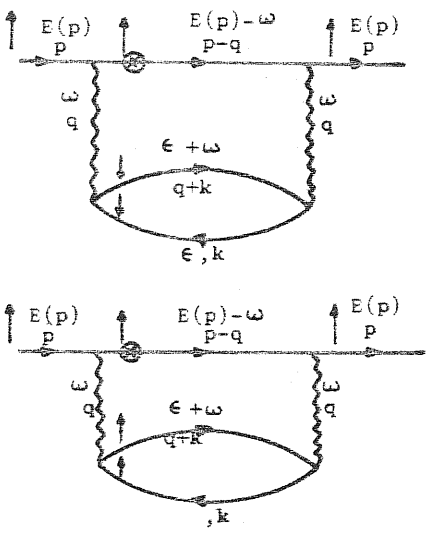

a)

b)

Fig.3. Diagrams associated with $R^{\uparrow}_{nf1}$-(a) and with $R^{\uparrow}_{nf2}$-(b) terms representing non-flip processes.

The $R^{\downarrow}_{f}$ and $R^{\downarrow}_{nf}$ quantities are calculated in a similar way. All the the results are shown in Ref. [7].

Knowing the flip and the non-flip scattering rates we can calculate probabilities per unit time $P^{\uparrow(\downarrow)}(E)$ for spin-up(down) electron with energy E that any inelastic scattering event occurs:

$$P^{\uparrow(\downarrow)}(E) = \int_0^E d\omega \left(R_f^{\uparrow(\downarrow)}(E,\omega) + R_{nf}^{\uparrow(\downarrow)}(E,\omega)\right) \tag{12}$$

3. Electron cascade: a classical "computer simulation"

As explained in the Introduction, neglect of quantum interference effects allows the discussion of the electron cascade in purely classical terms, thus available to direct computer simulation.

In our simulation an electron is considered as a point particle moving in space and time. Each electron above the Fermi level is kept track independently of others. The continuous trajectory of an electron is broken into "hops" of length Δl, which is chosen tentatively as one-sixth of the nearest neighbours spacing in iron crystal i.e. $\Delta l = .4\text{Å}$.

Let us consider now what happens for example to a spin-up electron. At the end of each "hop" the electron, with energy E, can suffer inelastic scattering. This happens with a probability P given by:

$$P = P^{\uparrow}(E)\Delta t \tag{13}$$

where $P^{\uparrow}(E)$ is given by (12), and

$$\Delta t = \Delta l / v^{\uparrow}(E) \tag{14}$$

and

$$v^{\uparrow}(E) = (2(E+E_F)/m)^{1/2} \tag{15}$$

$$\left[v^{\downarrow}(E) = (2(E+E_F-\Delta)/m)^{1/2} \right]$$

Clearly, when $\Delta l \to 0$ the mean-free-path (MFP) of electron would be the same as predicted by theory.

During inelastic scattering event spin-up electron with momentum $\underline{p}$ loses energy and transfers momentum $\underline{q}$ to the created electron-hole system. After this scattering there are two electrons above the Fermi level: one with momentum $\underline{p}-\underline{q}$ another with momentum $\underline{q}+\underline{k}$. Momenta $\underline{q},\underline{k}$ and spins of the electrons have to be chosen with proper probability.

Looking back to formulas (5),(7)-(11) and Fig.2 & Fig.3 one can notice that: the probability $P(\underline{p}^{\uparrow};(\underline{p}-\underline{q})^{\downarrow},(\underline{q}+\underline{k})^{\uparrow})$ that a spin-up electron with momentum $\underline{p}$ produces spin-up electron with momentum $\underline{p}-\underline{q}$ and spin-down electron with momentum $\underline{q}+\underline{k}$ is proportional to:

$$P(\underline{p}^{\uparrow};(\underline{p}-\underline{q})^{\downarrow},(\underline{q}+\underline{k})^{\uparrow}) \propto \frac{\theta(|\underline{q}-\underline{k}|-1)\theta((1-2\Delta)^{1/2}-k)}{((\underline{p}-\underline{q}-\underline{k})^2-q_{FT}^2)^2} \tag{16}$$

and, keeping the same notation:

$$P(\underline{p}^{\uparrow};(\underline{p}-\underline{q})^{\uparrow},(\underline{q}+\underline{k})^{\downarrow}) \propto \frac{\theta((1-2\Delta)^{1/2}-k)\theta(|\underline{q}+\underline{k}|-(1-2\Delta)^{1/2})}{(q^2+q_{FT}^2)^2} \qquad (17)$$

$$P(\underline{p}^{\uparrow};(\underline{p}-\underline{q})^{\uparrow},(\underline{q}+\underline{k})^{\uparrow}) \propto \theta(|\underline{q}+\underline{k}|-1)\theta(1-k)* \qquad (18)$$

$$*\left(\frac{1}{(q^2+q_{FT}^2)^2}+\frac{1}{((\underline{p}-\underline{q}-\underline{k})^2+q_{FT}^2)^2}-\frac{2}{(q^2+q_{FT}^2)((\underline{p}-\underline{q}-\underline{k})^2+q_{FT}^2)}\right)$$

θ functions insure that both electrons are above the Fermi level. Energy conservation requirement add one more condition for $\underline{q}$ and $\underline{k}$:

$$\underline{p}\cdot\underline{q}=\underline{q},\underline{k}+q^2 \qquad (19)$$

Similar formula can be written for scattered spin-down electron.

After this scattering, two electrons plus a hole with well-defined spin and momenta travel through the metal exciting eventually other electrons. In principle this cascade process is infinite and each electron which will not escape to the vacuum reaches the Fermi level through repeated inelastical scattering.

As a further approximation, we choose to neglect energy loss processes caused by the hole, and in particular the new electron hole pairs thus generated. Since the hole can only lose energy less than E_F, the chance that it can give rise to an electron with sufficent energy to be relevant is finite, but very small.

The only interesting electrons are for us those electrons which have a chance to cross the surface of the metal and "be observed" as secondaries. So, after inelastic scattering the energies of two electrons are checked and those with energy less than work function ϕ are no longer traced, since their only fate is to sink into the Fermi sea of conduction electrons.

Going through the crystal, an electron can reach the surface and after crossing it can be fixed as secondary electron with given energy, spin and momentum.

It can also happen that an electron approaches the surface from such a direction that the electron energy "perpendicular" to the surface is smaller than ϕ. In this case the electron is scattered elastically, i.e. it changes the sign of the momentum component perpendicular to the surface, and is sent back to the bulk. We neglect the possibility of the reflection for an electron with normal momentum component larger than $\sqrt{2m(E_F+\phi)}$. Such effect is important for electrons which tend to escape on trajectories close to the surface of the metal. As we have found it is only small part of all secondaries.

So far, we have not discussed at all elastic scattering by the crystal lattice potential. It is however well known [8] that the total yield of secondaries is mainly fixed by the elastic scattering. This is essentially because inelastic scattering is strongly peaked forward. While inelastic scattering is responsible for the final energy distribution, and (as we believe) for the state of polarization of secondaries, it does not deflect the electrons sufficiently to turn them back out of the surface with respectable intensity. On the other hand, elastic scattering does precisely this. It does in principle also spin-polarize the electrons. However, since we expect a much smaller number of elastic events than inelastic, we will neglect any polarizing effects here.

Elastic scattering is crudely introduced in our simulation in the following way. In the spirit of muffin-tin approximation we give each ion of the lattice a conventional radius or screening length λ, taken for Fe or Al to be one-fourth of the distance between nearest neighbours (for Fe $\lambda \sim 6$ Å).

If in the course of its movement the electron is closer to any atom than λ, the elastic scattering occurs. The probability $Q(\theta)$ for the electron with momentum $\underline{p}$ to be scattered in the angle θ is given by:

$$Q(\theta) \propto \frac{1}{(4p^2(\sin\tfrac{1}{2}\theta)^2+(2\pi/\lambda)^2} \qquad (20)$$

It should be pointed out that coherent effects, such as Bragg elastic diffraction are neglect entirely, as this is known to scatter backwards a total of perhaps only 5% of the total incident beam [8].

The elastic scattering as described above (20) has too an impact for small energy electrons. For small $\underline{p}$ $Q(\theta)$ becomes almost flat function of θ and electrons scattered isotropically have little chance to reach the vacuum. It affects mostly the flux of small energy secondaries. We have found that the efficency of the secondaries production fits best to the experimental data by allowing an elastic scattering to occur with probability $(1-\frac{E_F}{E+E_F})^2$.

For the time being we stay with this artificial treatment. We believe that the proper consideration of the electron as a wave packet scattered on the lattice interfering with itself would not change the picture cascade formation.

In the simulation the primary energy E_p (measured with respect to vacuum zero), the electron angle of incidence α (measured with respect to the surface normal) and the parameters of the metal are to be chosen at the begining. Each "experiment" consists of repeated injections of one electron with the same momentum $\underline{p}$ and with different spin orientation. A large number of primaries is needed for each simulation ($10^5 \div 10^6$) in order to achieve reasonably accurate values of yield and polarization of secondaries for energies below ~10eV.

Data of outgoing electrons (energy-measured with respect to vacuum zero, direction, spin orientation) are stored. Histograms can then be made, with one eV as the energy interval.

Errors are estimated by observation of the statistical fluctuations of the results with increasing number of primaries.

4. Paramagnetic metal

In a paramagnetic metal $\Delta=0$. We use generally $E_F=11.2$eV, and $\Delta=4.3$eV. These values of E_F and Δ are also very close to the parameters of aluminium: $E_F=11.7$eV and $\Delta=4.25$eV.

Fig.4 shows the results obtained for a preliminary run, with all primaries up-polarized, and electrons leaving the metal after one inelastic scattering only.

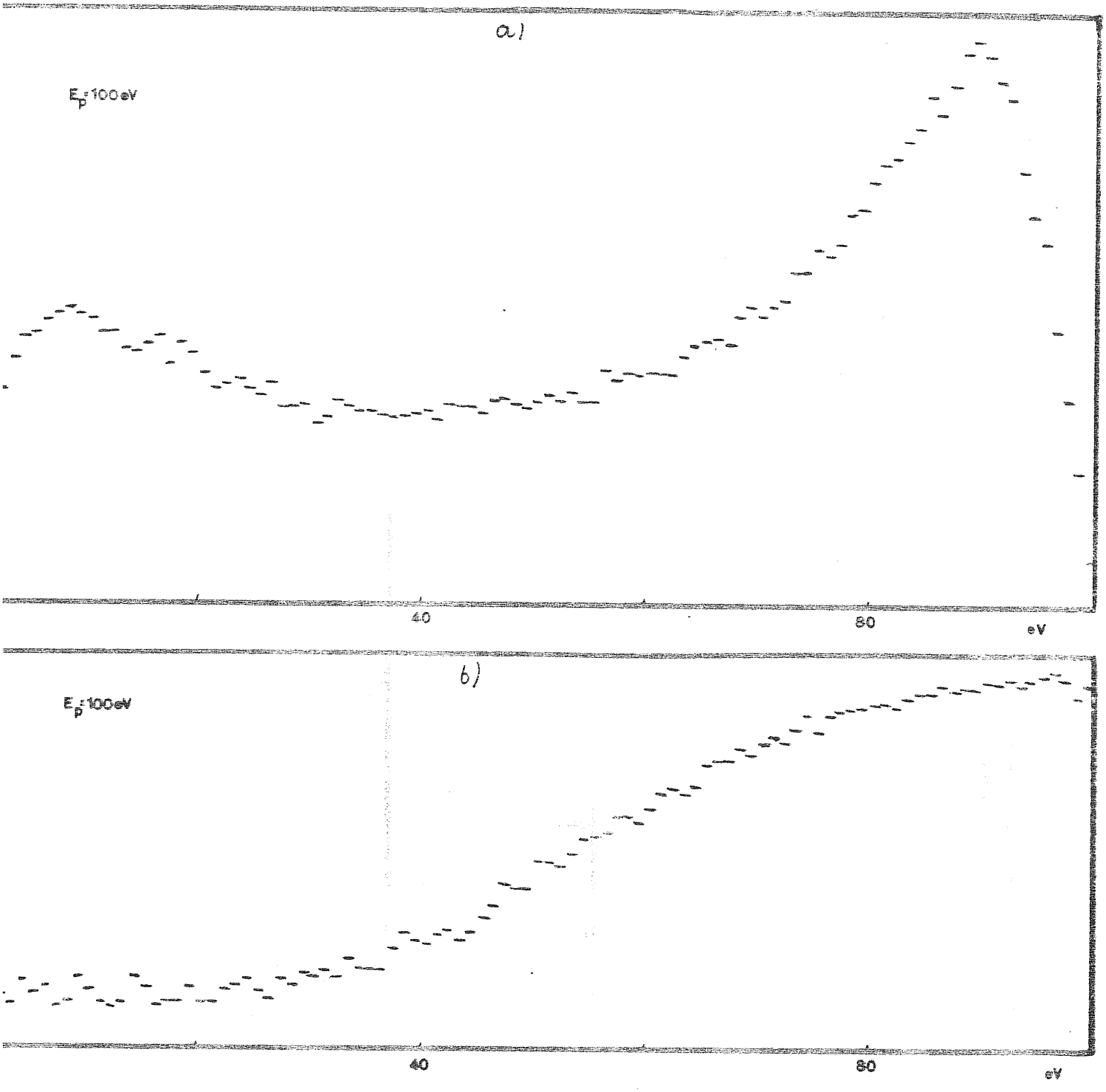

Fig.4. Intensity (a) and polarization (b) of electrons which left the metal after one inelastic scattering as a function of their energy.

As shown on Fig.4a the primaries tend to lose most frequently energy E_F. As discussed earlier, this can be thought as a particle-hole pair remnant of the plasmon peak (here absent because of the assumed static V(q)). It is caused by the growing number of electrons which can be excited while ω changes from 0 to E_F.

As we see on Fig.4b electrons which have lost energies up to E_p remain almost completely polarized. On the other hand low energy electrons, that have lost most of their primary energy, have acquired a polarization opposite to the original. This negative polarization can be understood as an exchange effect. Incoming spin-up primaries interact more strongly with spin-down than with spin-up electrons because of the Pauli principle, thus causing a slight excess of down electrons in the end.

The formation of cascade can be considered as the multiple convolution of the process described above.

Results of the complete simulation for scattering of 100%-polarized primaries are shown on Fig.5. The number of primaries was 200.000 . The overall efficency in secondary generation in this experiment is .8 . As one can observe multiple inelastic scattering shifts drastically the intensity of outgoing secondaries to small energies. Rather surprisingly, the negative polarization effect at low energies still ramains , although now the average number of scattering events is as high as 12, for E_p=100eV and α=30°.

We have also studied the dependence of the residual negative polarization P_N upon the primary energy E_p, the result is displayed in Fig.6. (Here P_N is defined as the polarization of electrons averaged on the energy range where the polarization is negative.)

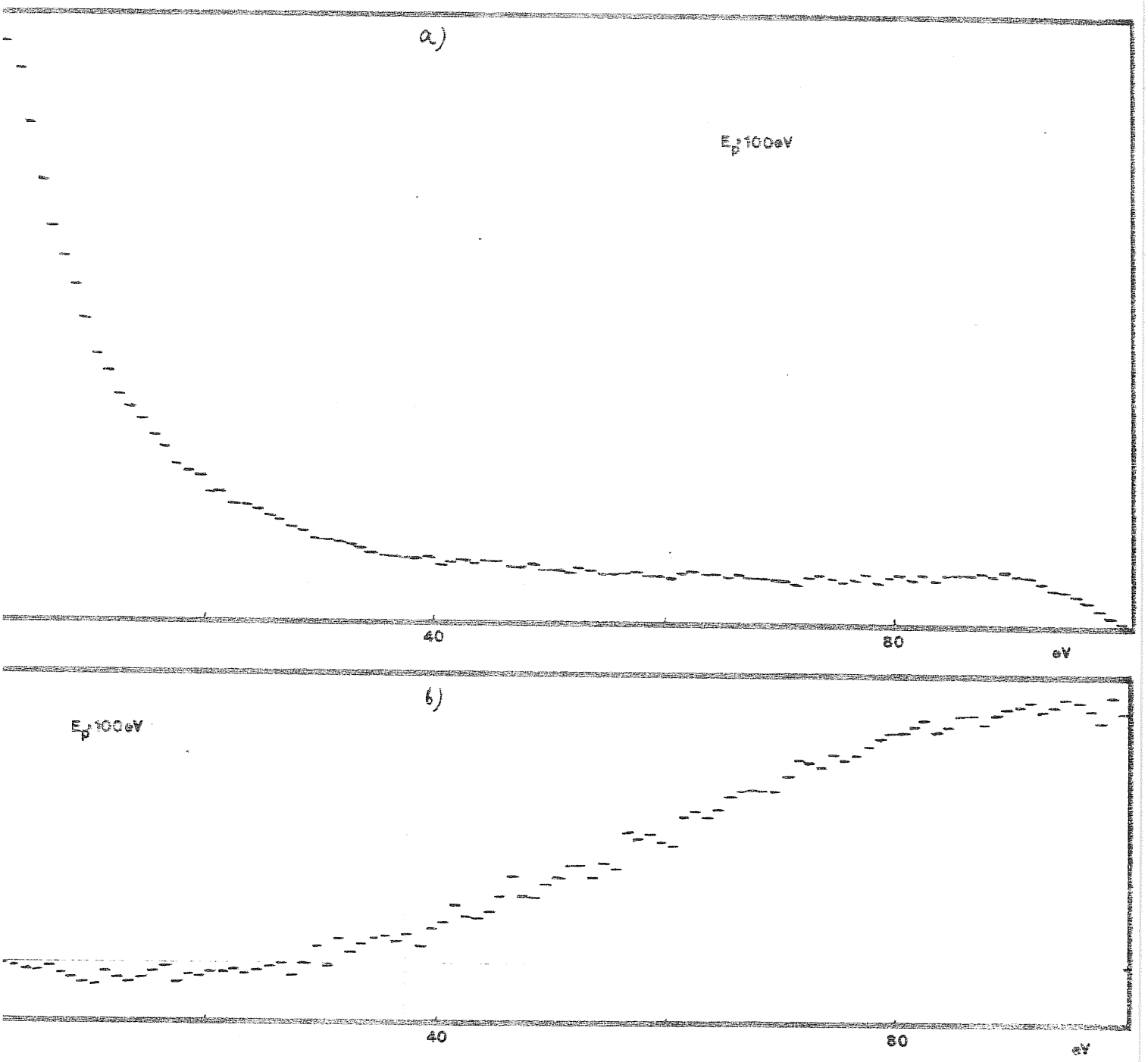

Fig.5. Intensity (a) and polarization (b) for completely polarized primaries with E_p=100eV, α=30°.

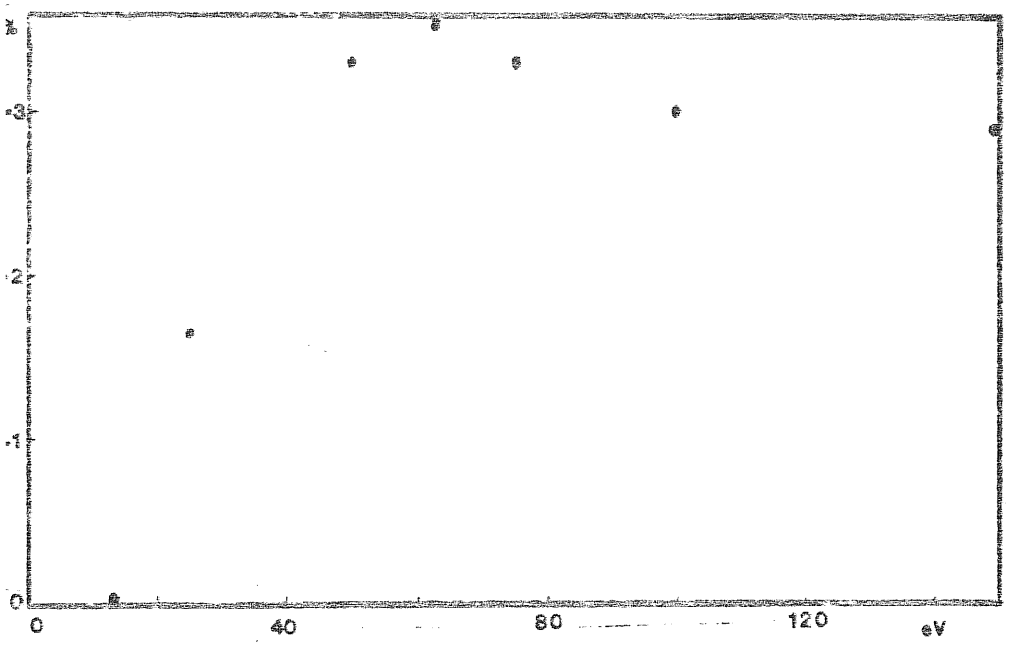

Fig.6. Average (negative) polarization P_N of low energy electrons as a function of primary energy Ep. The error of P_N is less than .1(%).

The appearence of a maximum for $|P_N(E_p)|$ is caused by two competitive effects.

Increasing of primaries energy E_p enlarges the cascade of secondaries and phenomenon of negative polarization shown on Fig.4 tends to wash out. For larger E_p electrons are scattered more and they " forget " about spin orientation of primary electron.

The decrease of E_p below 60eV switches on another mechanism. Highly polarized electrons with energies from the range below E_p (see Fig.4) start to cover energies where possibly negative polarization could appear. They suppress it completely for E_p less than 13eV.

There is however another experimental possibility for changing the size of secondaries cascade keeping E_p constant. This can be done by changing the incidence angle α.

For small values of α electrons have to suffer a relatively big number of inelastic scatterings until they turn back onto the metal surface. On the contrary, primaries injected at large angle α produce cascade almost parallel to the metal surface, and easy outgoing electrons are found, that have experienced only a small number of scatterings.

On Fig.7 we show intensity and polarization of secondaries for primary beam almost parallel to the metal surface. We choose E_p=63eV where $|P_N(E_p)|$ has its maximum.

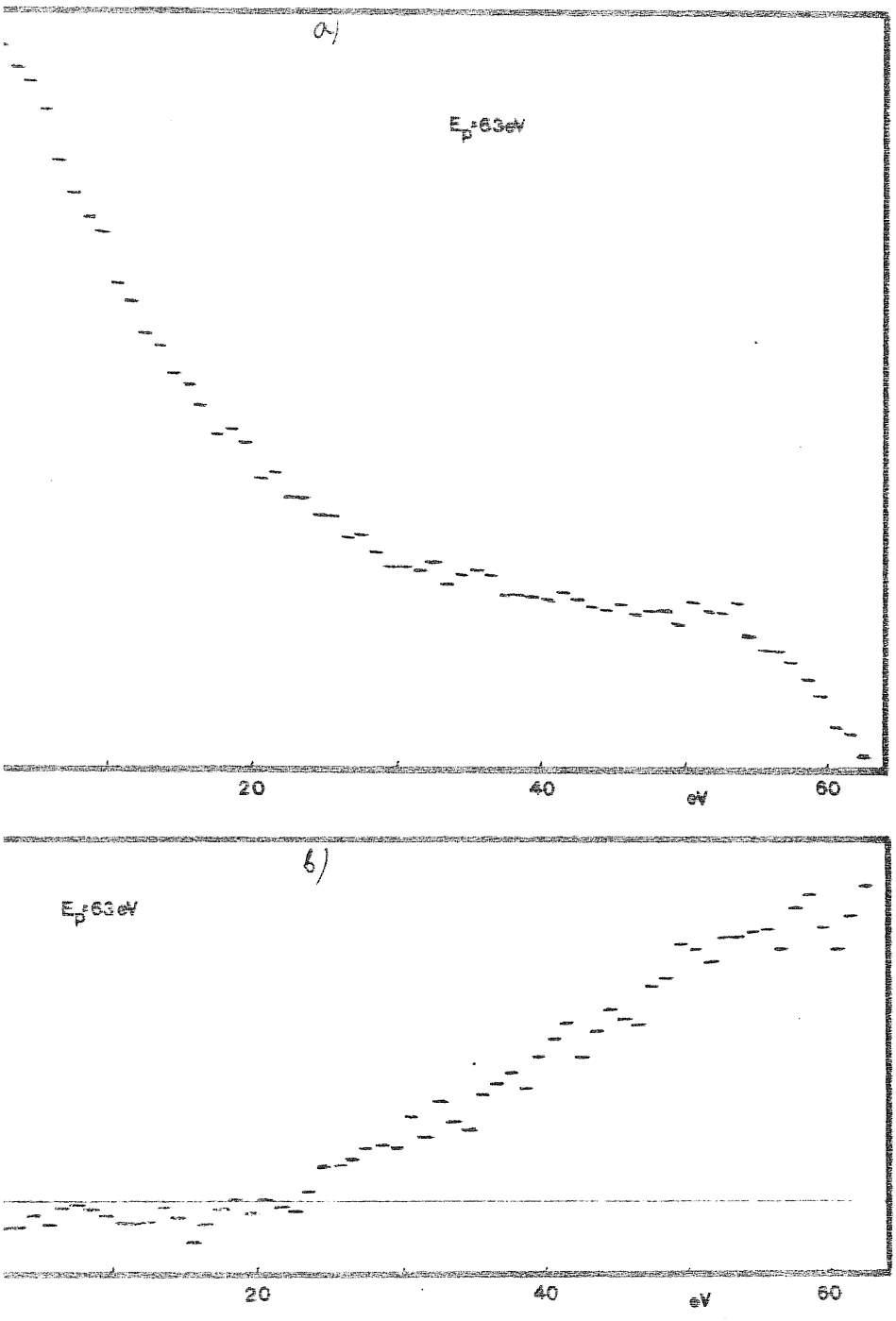

Fig.7. Intensity (a) and polarization (b) for completely polarized primaries with E_p=63eV, α=90°.

Here we find n_{ie}-defined as the average number of inelastic events per one incoming electron-equal to 6.2. This small number of inelastic scatterings is responsible for the increase of negative polarization with respect to the case shown on Fig.5b. The intensity shape (Fig.7a) is similar to that shown on Fig.5a, nevertheless it has also some resemblance to Fig.4a:the maximum (however very weak and broad) 11eV below E_p

and relatively high intensity of secondaries above low energy peak. Results presented on Fig.7 with n_{ie}=6.2 fall between the two previous ones with n_{ie} equal to 1. and 11.9 respectively.

Finally we show (Fig.8) the dependence of P_N on α with E_p constant and equal to 63eV.

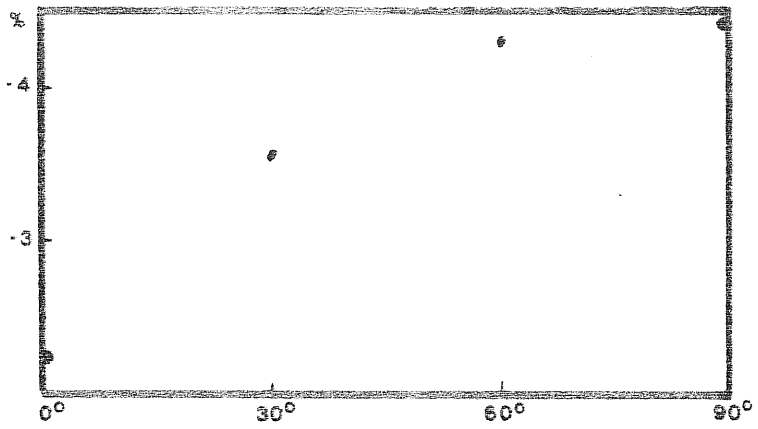

Fig.8. Negative polarization P_N as a function of α for E_p=63eV.

As one would expect P_N grows with α changing from 0° to 90°. Decreasing of α plays here with respect to P_N, the same role as increasing of primary energy discussed with connection to Fig.6. We find for α =0°,30°,60°, 90° n_{ie}=9.3; 8.0; 7.22; 6.22 which shows by itself the influence of α on the formation of secondaries.

The real experimental investigations for negative polarization of small energy secondaries would have also another advantage in the case of a big value of the angle α: the efficency (i.e. the total yield of secondaries divided by yield of primaries) is, as we find, almost twice as large for α~90° than for the incident beam normal to the surface of the metal.

In conclusion, we believe that negative polarization of secondaries could be usefully analysed in simple paramagnetic metals.

5. Ferromagnetic metal: secondary spin-polarization.

Modelling a ferromagnetic metal we choose Fe in the ferromagnetic phase where bulk polarization P_b=27%. Solving equations (1)-(4) one can find E_F=13.13eV and Δ=4.0eV . Note that this is a factor of two larger than the known exchange splitting of Fe. This is clearly due to inadequacy of our crude parabolic model to describe in detail that case. In this sense, all results of the present ferromagnetic case study are to be considered purely qualitative.

We have done computer simulation for E_p=400eV and α=30°. The results for intensity of outgoing electrons are shown on Fig.9.

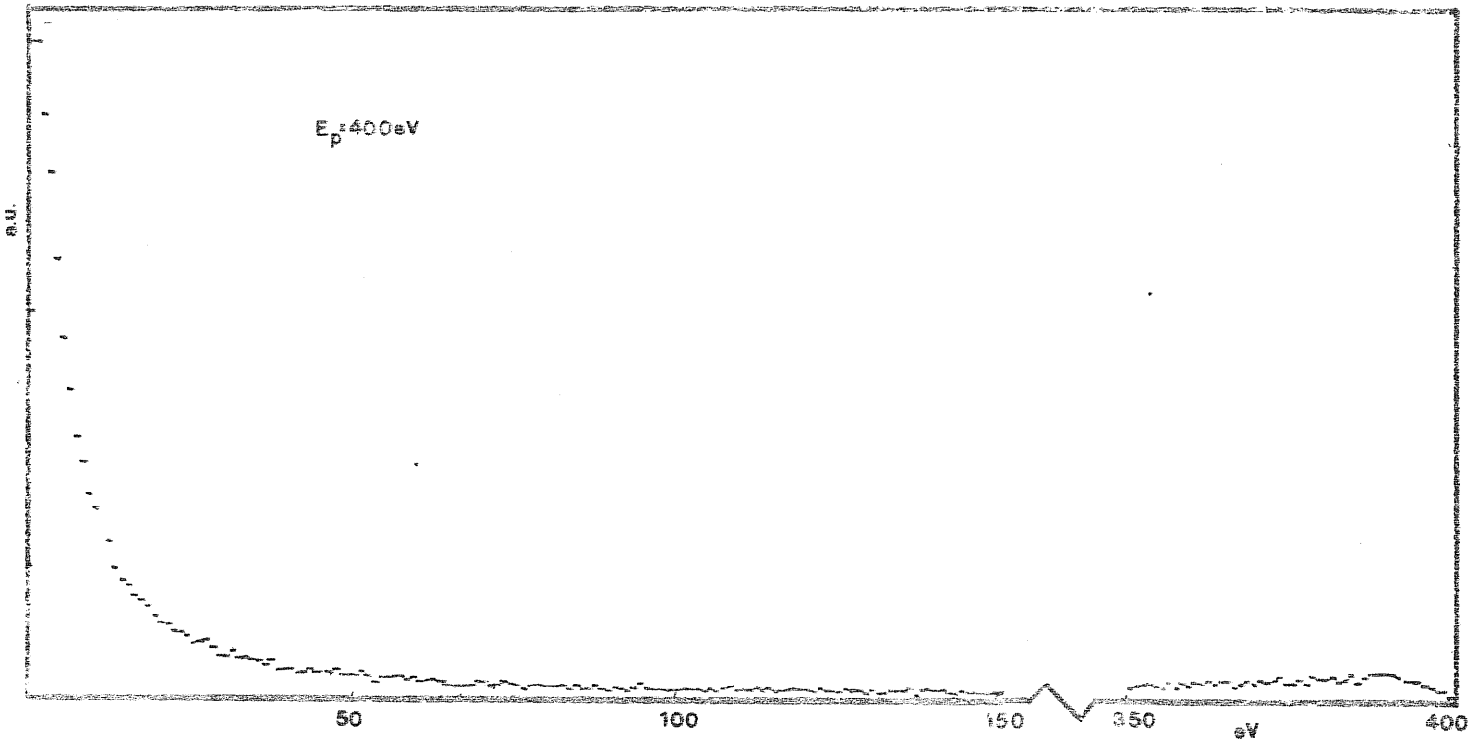

Fig.9. Intensity of secondaries as a function of their energy.

The shape of the intensity curve seems actually to agree well with experimental data [11] . One can notice also the shift of secondaries maximum to lower energy comparing Fig.9 with Fig.5a. The bigger E_p chosen for this case in fact implies more scattering events, here we find n_{ie}=44.7, and low energy electrons produced during cascade formation dominate secondaries energy spectrum. We expect the same n_{ie} dependence on incidence angle α as presented in the previous chapter and we have not verified it.

Total yield of outgoing electrons is 1.4 per incoming electron. About 13% of outgoing electrons have been backscattered elastically.

On Fig.10 the intensity and polarization of secondaries in low energy region is presented.

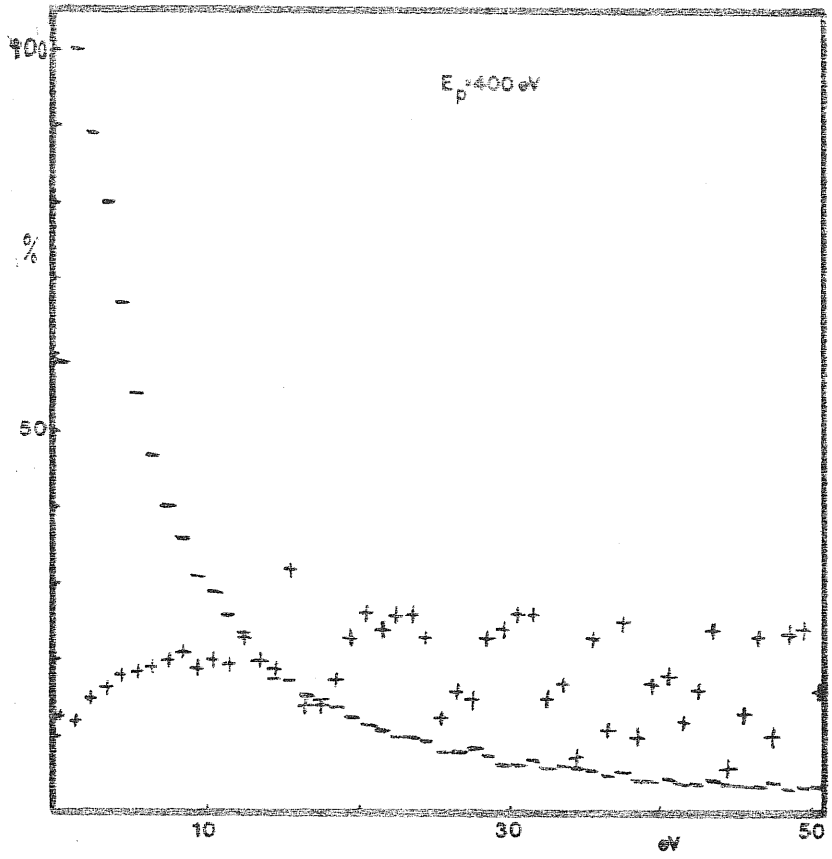

Fig.10. Polarization (+) in percent and intensity (-) in arbitrary units of secondaries as the function of their energy.

The error in polarization caused by statistical fluctuations is less than 1% for secondaries with energy up to 10eV (i.e. polarization for 10eV is equal 20.($\pm$1)%). The error grows with increasing secondaries energy because of the rapid decrease in the number of outgoing electrons.

We have not found any pronounced polarization angular dependence on the direction of outgoing electrons. The average polarization of all outgoing electrons is 12.4%, the average polarization of electrons leaving the metal in the direction within 15° to its surface is 13.1% .

Recent experimental data - that partly motivated this study - show a very different behaviour, with polarization rising up to about twice the bulk value for very low energy secondaries. The maximum polarization reported for 400eV primaries scatterred on the ferromagnetic iron is about 45% . Our secondary polarization lies generally below the bulk value.

We envisage at least two possible reasons for this discrepancy. One could be the total absence of flat d-bands near E_F in our model. However, it is not clear how inclusion of this feature could account for a high secondary electron polarization.

A second possibility is that the observed polarization rise could be a surface effect, which is again beyond our simple model. A surface mechanism would suggest a strong dependence of secondary polarization upon surface quality, and also upon the angle of emission, and there seems to be some evidence for both of this effects [12].

This leaves however the field wide open for theoretical investigation.

6. Ferromagnetic metal: asymmetry of mean-free-paths, versus spin-flip

The technique used in the presented work gives the opportunity for direct checking of spin dependence of mean-free-path (MFP) between inelastic events and its influence on polarization of secondaries.

One can see that there is a simple connection between MFP of spin-up (down) electron $\lambda^{\uparrow(\downarrow)}$ and $P^{\uparrow(\downarrow)}(E)$ defined by equation (12). Since $P^{\uparrow(\downarrow)}(E)$ is the probability per unit time that any inelastic event occurs $\lambda^{\uparrow(\downarrow)}$ is given by:

$$\lambda^{\uparrow(\downarrow)}(E) = \frac{v^{\uparrow(\downarrow)}(E)}{p^{\uparrow(\downarrow)}(E)} \qquad (21)$$

The values of $\lambda^{\uparrow}$ and $\lambda^{\downarrow}$ are on Fig.11 .

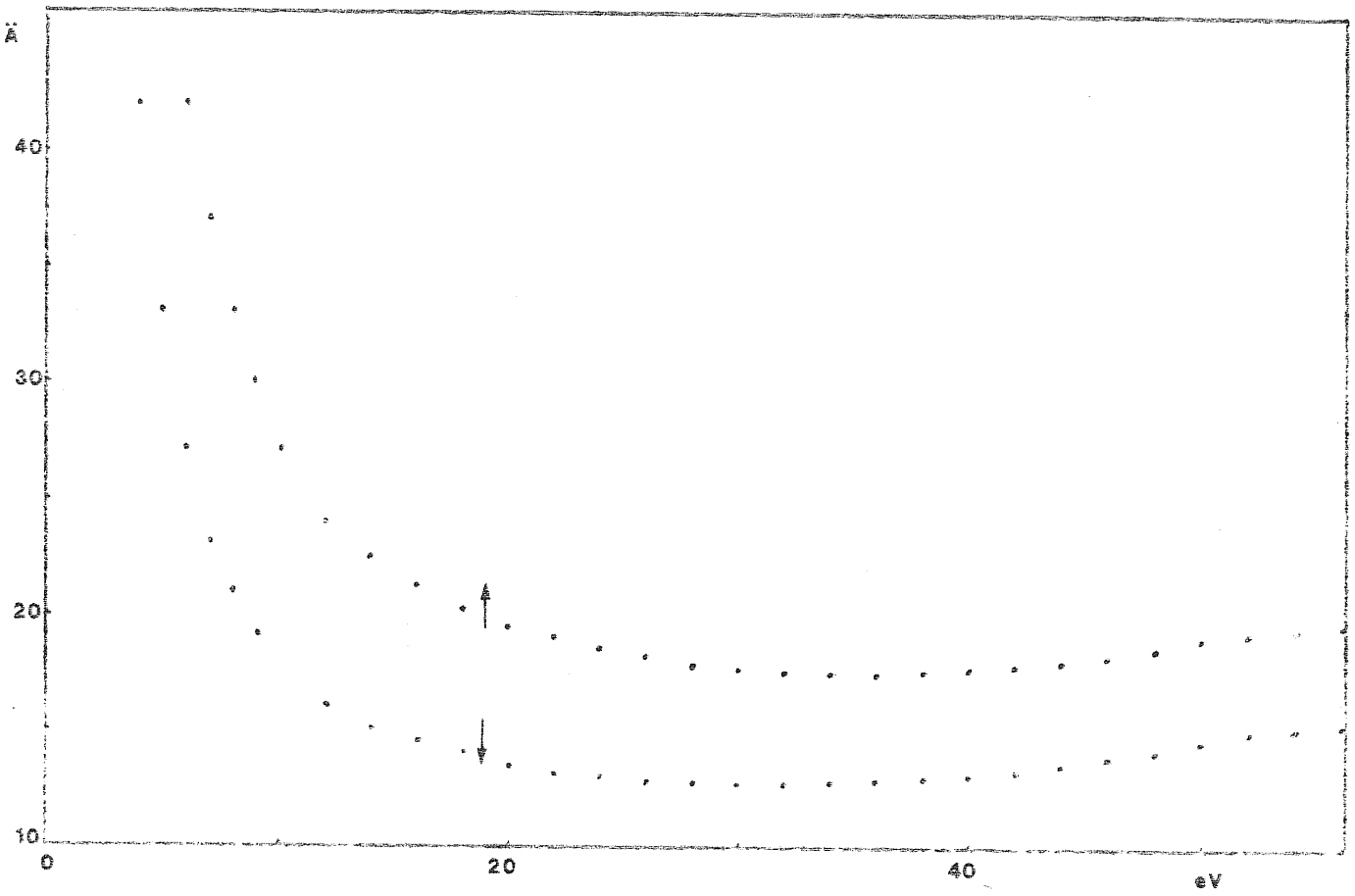

Fig.11. MFP of spin-up and spin down electron as a function of its energy in ferromagnetic iron with majority spin-up electrons.

In our approximation MFP of spin-up is always bigger than of spin-down electron. This inequality can be understood as the effect of exchange part of the interaction between electrons which tends to diminish this coupling. The spin-up electron "feels" more exchange interactions than spin-down one, because in the material there is more spin-up than spin-down electrons. Though a spin-down electron interacts more strongly with a cloud of conduction electrons and its MFP is shorter than for a spin-up one.

This type of result was anticipated by Bringer at al. [13] and Feder [14], who, however, greatly overestimated the magnitude of the effect. Our results are in disagreemant with those presented by Rendell and Penn [15]; in their findings the $\lambda^{\downarrow}(E) > \lambda^{\uparrow}(E)$ inequality is hold for small energies. We agree with Matthew's criticism [16] of this reversal inequality.

Below (Fig.12) we present results of computer simulation of electrons scattered on paramagnetic iron ($\Delta=0$), but with artificially introduced difference between MFP of spin-up and spin-down electrons. Values of MFP are taken from ferromagnetic metal (see Fig.11).

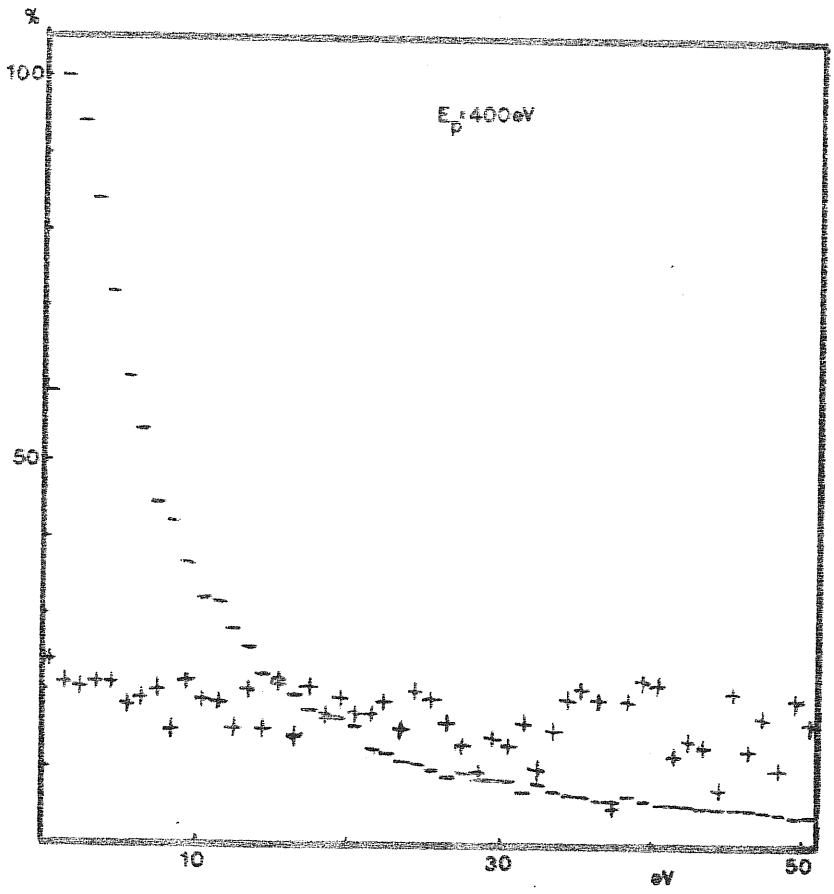

Fig.12. Polarization (+) in percent and intensity (-) in arbitrary units of secondaries for paramagnetic material with spin-dependent MFP.

Due to poorer statistics the errors in polarization are less than 1% for secondaries energy below 5eV, and higher energies should be disregarded.

On Fig.10 we had given the results of the "full" simulation where electrons have spin-dependent MFP and can also undergo spin-flip. Here on Fig.12 everything is rather similar, but spin-flip asymmetry is absent. The difference in polarization between Fig.10 & Fig.12 is not dramatic. The average polarization of outgoing electrons (Fig.12) is 11.1% which is only 1.3% less than for "full" simulation (Fig.10). The polarization up to 5eV, as shown on Fig.12, is even a little bit bigger than on Fig.10.

We conclude that spin-flip does not play a major role in secondary spin polarization (at least to the "bulk" part discussed here), and that MFP asymmetry is sufficient to explain the qualitative aspects of our result. This MFP asymmetry due to Pauli principle, has the opposite sign to that found by Rendell & Penn, and the same sign as that originally proposed by Bringer & Feder, although of smaller magnitude.

References

1. P.A. Wolff, Phys. Rev. 95, 56 (1954)
2. H.C. Siegmann, D.T. Pierce, and R.J. Celotta, Phys. Rev. Lett. 46, 452 (1981)
3. J. Unguris, D.T. Pierce, A. Galejs, and R.J. Celotta, Phys. Rev. Lett. 49, 72 (1982)
4. E. Kisker, W. Gudat, and K. Schröder, Solid State Com. 44. 591 (1982)
5. H. Hopster, R. Raue, E. KIsker, G. Güntherodt and M. Campagna, Phys. Rev. Lett. 50, 70 (1983)
6. S. Yin, E. Tosatti, ICTP 81/129
7. S. Yin, E. Tosatti, J. Glazer, to be published
8. J.B. Pendry, Low Energy Electron Diffraction, London & New-York Academic Press, 1974
9. A.L. Fetter, and J.D. Walecka, Quantum Theory of Many-Particle Systems, New York McGraw Hill, 1971
10. J.S. Eelman, and W. Baltensperger, Phys. Rev. B23, 1300 (1980)
11. H. Hopster, private information
12. J. Unguris, M. Campagna, private communication
13. A. Bringer, M.Campagna, R. Feder, W. Gudat, A. Kisker, and E. Kulhman, Phys. Rev. Lett., 42, 1705 (1979)
14. R. Feder, Solid State Com., 31, 821 (1979)
15. R. Rendell, and David R. Penn, Phys. Rev. Lett. 45 , 2057 (1980)
16. J.A.D. Matthew, Phys. Rev., B25, 3326 (1982)